

Influence of Cooling Rate on Crystallization of Borax in Stirred Batch Crystallizer

Marija Ćosić*, Anđela Pažin, Antonija Čelan, Nenad Kuzmanić

University of Split, Faculty of Chemistry and Technology, Department of Chemical Engineering, Ruđera Boškovića 35,
21000 Split, Croatia
akrap@ktf-split.hr

The aim of this work was to determine the influence of cooling rate on the nucleation and crystal growth of borax decahydrate. All experiments were carried out in baffled stirred crystallizer with the volume of 2.14 dm³. Mother liquor saturated at 30 °C was cooled down at 3 different cooling rates in the range from the 4 to 9 °C/h. In order to analyze and compare the influence of fluid flow pattern in the crystallizer on product properties, examinations were performed using two different impeller types; radial straight blade turbine (SBT) and axial pitched blade turbine (PBT). Mixing with both of impellers was carried out at constant impeller speed of 300 rpm. Concentration of the solution was measured in line by potentiometric method, while the changes of crystal size over process time were determined by optical microscope and image analysis software. The nucleation and crystal growth behaviors for borax–water system in a batch cooling crystallizer were estimated according to Mersmann's criteria. From the results obtained, it was found that cooling rate has great impact on nucleation and crystal growth kinetics. Moreover, in all system investigated nucleation was heterogeneous and crystal growth integration limited, its rates differed with cooling rates. The changes of those parameters with cooling rates in the systems with radial and axial impeller were similar. Nucleation and crystal growth reflected on the crystal size distribution as well. Increasing cooling rate crystal mean size decreases while crystal agglomeration increases, indicating the importance of cooling rate of batch crystallizer in the production of the crystals of desired properties.

1. Introduction

Crystallization refers to the phase transformation of a compound from a fluid or amorphous solid state to a crystalline solid state. Crystallization is usually analysed through its two main steps; nucleation and crystal growth. Kinetics of both steps governs crystal size distribution of the product. For crystallization to occur the system must be supersaturated and crystallization method is primarily selected according to the crystallizing compound solubility data. Cooling crystallization is adequate for salt which solubility increases with temperature. In this case, the cooling needs to be selected in the way it prevents uncontrolled nucleation and high supersaturation accumulation, which may lead to secondary nucleation and agglomeration. If saturated solution is cooled the supersaturation will gradually increase, but formation of solid phase in the solution only occurs when a certain degree of supercooling provides required supersaturation to initiate nucleation (De Haan and Bosh, 2013). This region of supercooling, i.e. of supersaturation is called metastable zone. Information about width of this zone presents essential information for crystallization kinetics. The aim of this work was to analyze the influence of cooling rate on nucleation and crystal growth kinetics as well on properties of borax crystals obtained in the investigation conducted. Borax decahydrate presents on of the most important boron compound which has wide variety of uses in all branches of process industry. Crystallization presents predominant operation in its production from tinkal ore. Obtaining the product of desirable characteristics like crystal purity, morphology and size is very important to define the influence of process parameters on crystallization, one of them is cooling rate.

2. Materials and Methods

All experiments in this work were carried out in apparatus presented in previously published paper (Ćosić et al., 2016). Crystallizer was a flat bottomed glass vessel with diameter $d_T = 14$ cm equipped with four baffles of standard dimension ($w = 1/10 d_T$). Liquid height, H , in the crystallizer was equal to vessel diameter. Crystallizer was immersed in thermostatic bath whose temperature was controlled by Huber Variostat CC3. Mixing in the crystallizer was performed by Lightnin LabMaster torque meter and turbine impeller. During examination two different four bladed impellers were used; straight blade turbine and pitched blade turbine with impeller to tank diameter $D/d_T=0.46$ and impeller off-bottom clearance, $c/H=0.33$. In all experiments impeller speed was kept constant $N = 300$ rpm. In this work solutions of disodium tetraborate decahydrate (borax) p.a. (Kemika, Croatia) saturated at 30°C were crystallized from its aqueous solutions by linear cooling to 5°C . Cooling rates were 4, 6 and 9°C/h . Concentration inside the crystallizer was monitored by potentiometric method, i.e. using sodium ion-selective electrode in combination with Ag/AgCl referent electrode. Details about usage of this method in a batch cooling crystallizer were described in details in above cited work.

Upon nucleation, a sample of the suspension was withdrawn from the system periodically in order to analyse the change of crystal size over process time. The withdrawal of the crystal magma was conducted from a fixed position, defined by the liquid height of $z/H = 0.8$ and the distance between impeller shaft and vessel wall expressed by the ratio $l = (d_T/2) = 0.4$. After sampling, crystals were sized using the Carl-Zeiss optical microscope and image analysis software (Motic Images Advanced 3.2). Upon completion of the process, crystals were filtered, washed with acetone, and then dried at room temperature. Obtained product was sieved through a series of Fisher's U.S. standard sieves. Crystal size distribution is presented by distribution function.

3. Experimental Results and Discussion

3.1. Influence of Cooling Rate on Metastable Zone Width and Nucleation Rate

Metastable zone width (MSZW) may be expressed as maximum allowable supercooling, ΔT_{\max} , or maximal allowable supersaturation Δc_{\max} . In this work, values of MSZW were estimated from the absolute supersaturation, which is a measure of the difference between the actual, c , and saturated concentration, c^* , of the mother liquor, ($\Delta c = c - c^*$). The changes of supersaturation over process time in the solution saturated at 30°C and cooled by applied linear cooling rate are given on Figure 1 for systems agitated by axial and radial turbine impeller.

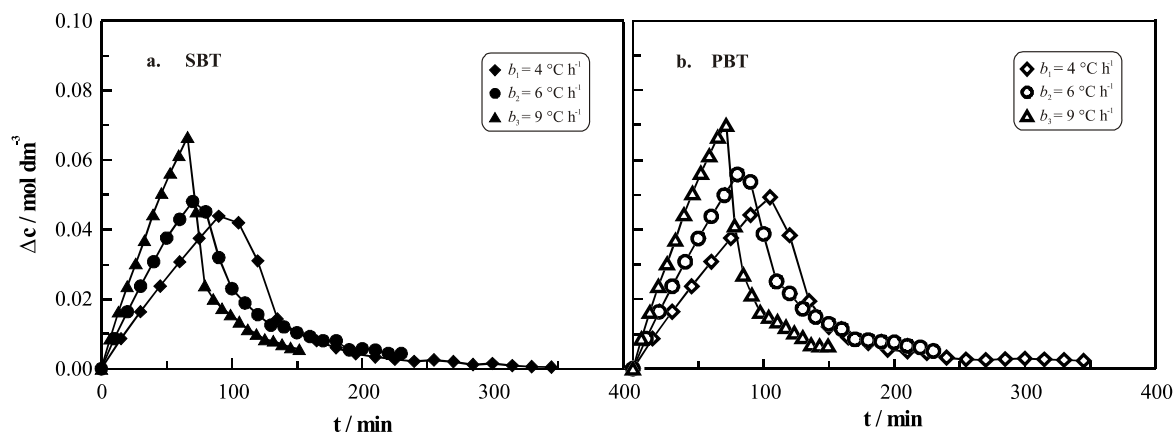


Figure 1. Supersaturation changes at different cooling rate and impeller speed of 300 rpm in: a. SBT impeller system, b. PBT impeller system

From the Figure 1 it can be seen that supersaturation changes over process time presents a similar trend; at the beginning supersaturation linearly increases, reaches the maxima and then decreases. Linear supersaturation increment depends on cooling rate, so the slope of this part of the curve, is identical for the same cooling rate in axial and radial systems. Maximal value of supersaturation presents metastable zone width, Δc_{\max} , i.e. maximal allowable supersaturation at which nucleation started. From the results, it is clear that this parameter increases with cooling rate, and it reaches the highest value at 9°C/h in the both systems. By deeper analysis of those results it can be seen that fluid flow pattern inside the crystallizer generated by axial and radial impeller have also an impact on MSZW. It is slightly lower in SBT impeller system for the

same cooling rate. However, from the results it is evident that cooling rate has much more prominent effect on MSZW than fluid flow pattern generated inside the crystallizer at the same impeller speed. Decrement of supersaturation is consequence of desupersaturation due to crystal growth and secondary nucleation that will be discussed latter during crystal growth analysis.

The nucleation rate is proportional to metastable zone width and many correlations were proposed between nucleation rate and MSZW. The rate of nucleation, B , is the sum of the four contributions of different mechanisms; homogeneous nucleation, B_{hom} , heterogeneous nucleation, B_{het} , secondary surface nucleation, B_{sur} , attrition induced secondary nucleation, B_{att} . Kim and Mersmann (2001) assumed that at certain supersaturation one mechanism becomes dominating and they suggested nucleation criterion which presents dimensionless metastable supersaturation $\Delta c_{\text{max}}/c_c$ vs. dimensionless solubility c^*/c_c diagram, where c_c is molar crystal density. In Mersmann's nucleation criterion shown in Figure 2a experimental data obtained in this investigation were marked by symbols. It was found that the heterogeneous primary nucleation is the dominating mechanism in all systems examined. In this case the heterogeneous nucleation rate can be calculated by the following equation (Mersman, 1994):

$$B_{\text{het}} = 0.965 \varphi_{\text{het}} \frac{D_{\text{AB}}}{d_m^5} \left(\frac{\Delta c_{\text{max}}}{c_c} \right)^{7/3} \sqrt{f \ln \frac{c_c}{c^*}} \exp \left[-1.19 f \frac{[\ln(c_c / c^*)]^3}{(\eta \ln S)^2} \right] \quad 1$$

where φ_{het} is the heterogeneity factor and f is the reduction factor for the nucleation work. For heterogeneous nucleation $0 < f < 1$, and depends on the contact angle between the surface of the foreign particles and surface of the nucleus. D_{AB} is a bulk diffusivity ($= 10^{-10}$ m²/s in the low viscous solutions) and $d_m = (c_c/N_A)^{-1/3}$ where N_A is Avogadro number. The calculation was carried out with $D_{\text{AB}} = 3.94 \times 10^{-10}$ m²/s, $c_c = 4.48$ mol/dm³ which was valid for estimated parameters of $\varphi_{\text{het}} = 10^{-11}$ and $f = 0.1$. Numerical values of calculated rates of primary heterogeneous nucleation rate are given in Table 1.

Results indicated that rate of nucleation is proportional to the metastable zone width; it increases with cooling rate and it is higher in axial impeller system.

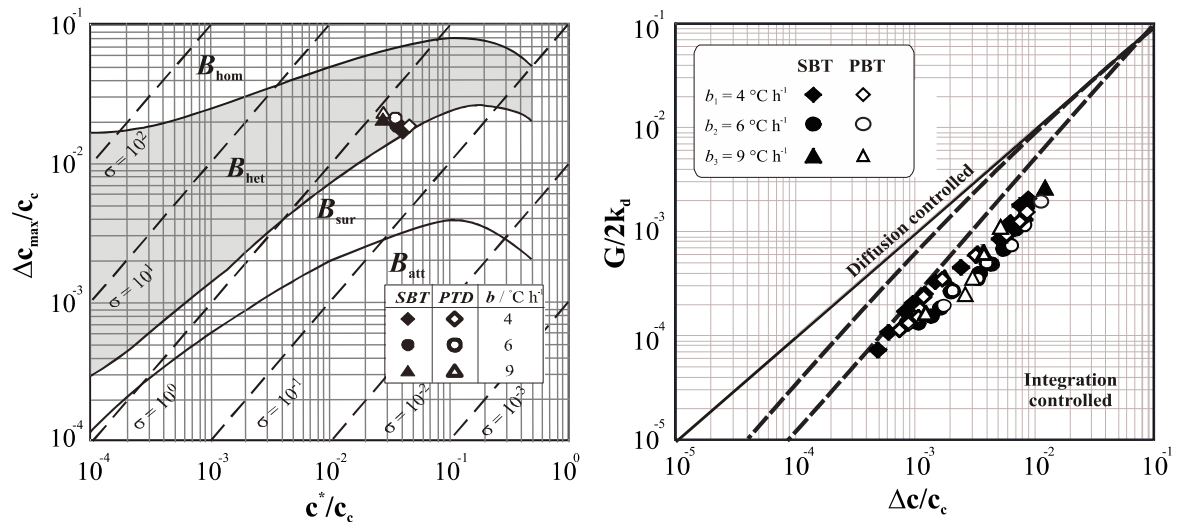


Figure 2: a. Mersmann nucleation criterion (Kim and Mersmann, 2001); b. Dimensionless crystal growth rate vs. dimensionless supersaturation

Table 1: Values of nucleation rate at different cooling rate in SBT and PBT system

	SBT	PBT
b/ °C/h	$B_{\text{het}}/ \text{No.}/ \text{m}^3 \text{ s}$	$B_{\text{het}}/ \text{No.}/ \text{m}^3 \text{ s}$
4	$4.88 \cdot 10^{16}$	$7.20 \cdot 10^{17}$
6	$4.64 \cdot 10^{17}$	$2.09 \cdot 10^{18}$
9	$1.98 \cdot 10^{19}$	$2.05 \cdot 10^{19}$

3.2. Influence of Cooling Rate on Crystal Growth Rate and Mechanism

Changes of linear crystal sizes, L , of growing crystals over process time, after the onset of nucleation, at different cooling rate are given in Figure 3 for radial and axial impeller systems. Linear crystal size presents average size of $n = 50$ largest, regular shaped crystals with linear size, L_c . The crystals were withdrawn from the crystallizer and analysed according to previously described procedure. Linear crystal size was calculated according to equation:

$$L = \frac{L_c}{n} \quad (2)$$

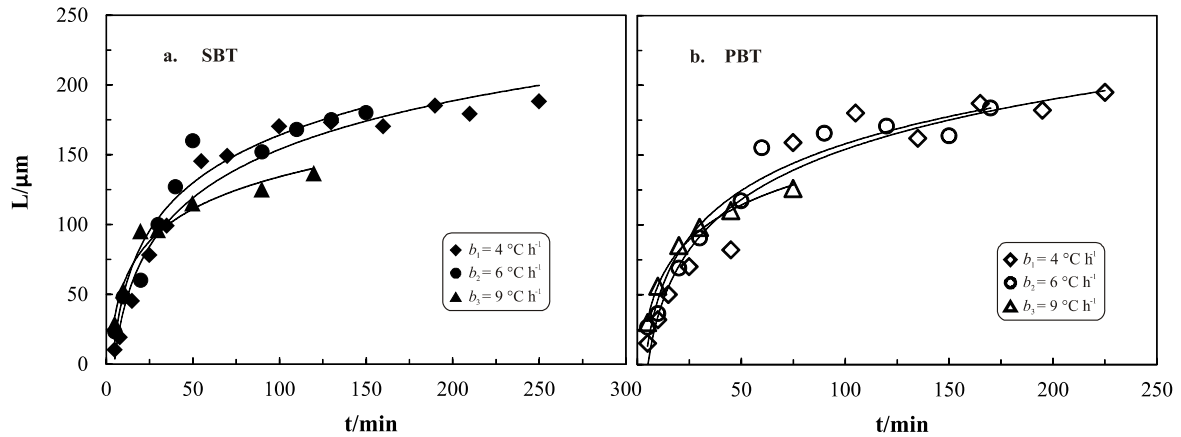


Figure 3. Variation of linear crystal size over process time at different cooling rate in the system: a. with SBT impeller and b. PBT impeller

Since crystallization is conducted from 30 °C to 5 °C, the longest process time was at cooling rate of 4 °C/h. Due to longest retention time of growing crystals inside the magma, at this cooling rate, final size of borax crystals was largest, in both systems. On the other hand, final size of borax crystals obtained at 9 °C was the smallest. Along with linear crystal size here will be also analysed supersaturation of the mother liquor presented in Figure 1. From supersaturation changes, it can be seen that desupersaturation is less pronounced at lower cooling rates. Less pronounced desupersaturation and more pronounced size increment may indicate that in this system supersaturation have been mostly consumed during the growth of nuclei generated by primary nucleation. Since that in the systems with the highest cooling rate a reverse trend is present it can be expected that here supersaturation is consumed not only on the large number of nuclei formed by primary nucleation but also on formation of secondary nuclei. Whether these assumptions will be accurate will only be seen after the analysis of size distributions of the borax crystals upon the processes finalisation.

Crystal growth consists of several steps, which are summarized in two main step process; volume diffusion and surface integration of the solute to the crystal lattice (Cheon et al., 2005; Mersmann, 1995). The growth rate is limited by the slower step that may change with a change in supersaturation and temperature. In this work crystal growth rate is expressed as linear growth rate calculated from the changes of linear crystal size over process time:

$$G = \frac{dL}{dt} \quad (3)$$

Experimentally determined crystal growth rates were marked in dimensionless crystal growth rate vs. dimensionless supersaturation diagram proposed by Mersmann (1995) and presented in Figure 2b. In this diagram k_d appears, being a mass transfer coefficient determined by equation proposed by Herndl (1982):

$$k_d(L) = \frac{D_{AB}}{L} \left[0.8 \left(\frac{\varepsilon \cdot L^4}{\eta_L^3} \right)^{0.2} \left(\frac{\eta_L}{D_{AB}} \right)^{0.33} + 2 \right] \quad (4)$$

where ε is the mean specific power input. This parameter is calculated from the experimentally determined power number and geometrical characteristics of the crystallizer and its values for SBT and PBT systems (at Reynolds number, $N_{RE} \approx 21600$) are 2.33 and 1.15 respectively. Parameter P^* presents a curve fitted to the crystal growth rates data at which the two mechanisms of crystal growth, volume diffusion and integration to the crystal lattice, are superimposed. In this work values of parameter P^* are below 10^{-5} . This parameter is a function of mass transfer coefficient, molar density, volume diffusion coefficient, solubility and molecular diameter. All mentioned parameters are calculated according to the procedure given in previously published paper (Kačunić et al. 2017).

In the figure 2b is clear that crystal growth rates are integration controlled at all cooling rates regardless impeller applied. This is even more pronounced at highest supersaturation generated in systems with highest cooling rate ($b = 9 \text{ }^\circ\text{C/h}$).

3.3. Crystal Size Distribution obtained at Different Cooling Rates

In order to analyse the influence of cooling rate on crystal properties on the Figure 4 is shown crystal size distributions of final product obtained at applied cooling rates in SBT and PBT impeller system.

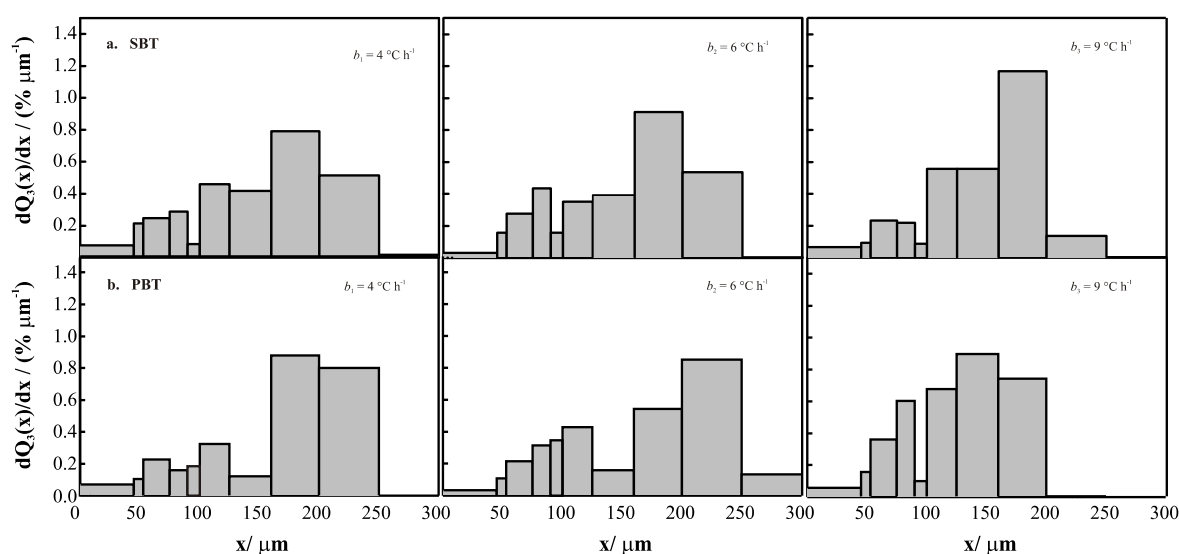


Figure 4: Crystal size distribution of borax obtained at different cooling rate in a system with a. radial impeller b. axial impeller

Fraction of fines (size $x < 100 \text{ } \mu\text{m}$) indicated the presence of secondary nucleation in all systems investigated and that this phenomena is the highest in PBT impeller system with highest cooling rate. Fraction of coarse crystals which can be result of crystal growth or agglomeration at 4 and $6 \text{ }^\circ\text{C/h}$ are very similar in both impeller systems. On the other hand, at $9 \text{ }^\circ\text{C/h}$ coarsest crystal fraction in SBT impeller system decreases, while in PBT impeller system the maxima in coarse fractions moved toward the smaller sizes. The facts mentioned have caused that the value of crystal weight mean diameter, x_m , are very similar at 4 and $6 \text{ }^\circ\text{C/h}$ and it is smaller at $9 \text{ }^\circ\text{C/h}$ in both system investigated (Table 2). The values of weight mean diameters, x_m , and standard deviations of crystal size, σ , were calculated according the procedure in previously published paper (Akrap et al., 2012). Microscopic analysis showed that crystals of coarsest fraction obtained by the lowest applied cooling rate are more regularly shaped than those obtained at higher cooling rate. Coarse crystals obtained at $9 \text{ }^\circ\text{C}$ are mainly result of agglomeration regardless of impeller type applied.

Table 2: Values of weight mean diameter and standard deviation of crystal size at examined cooling rates

b/ $^\circ\text{C/h}$	SBT		PBT	
	$x_m/\mu\text{m}$	$\sigma/\mu\text{m}$	$x_m/\mu\text{m}$	$\sigma/\mu\text{m}$
4	160	57	175	56
6	164	55	178	61
9	151	46	145	42

4. Conclusions

Metastable zone width of borax dehydrate significantly depends on cooling rate and it increases as cooling rate increases. This reflected on the nucleation mechanism and nucleation rate. In all system investigated, nucleation occurred by heterogeneous primary nucleation mechanism. The rate of heterogeneous nucleation was proportional to metastable zone width; it increased with cooling rates and was slightly higher in radial impeller systems. Crystal growth in all system investigated was integration controlled, especially at higher supersaturation generated at higher cooling rates. Crystal size enlargement was more emphasised at lower cooling rate due to longer retention time and moderate desupersaturation. Crystal size distribution indicated that although in all system investigated secondary nucleation was present in systems with higher cooling rates agglomeration became more pronounced. It is possible to produce large and regularly shape crystals at lowest cooling rates regardless of impeller type in the crystallizer.

References

- Akrap M., Kuzmanić N., Prlić Kardum J., 2012, Impeller geometry effect on crystallization kinetics of borax decahydrate in a batch cooling crystallizer, *Chemical Engineering Research and Design*, 90 (6), 793-802.
- Ćosić M., Kaćunić A., Kuzmanić N., 2016, The investigation of the influence of impeller blade inclination on borax nucleation and crystal growth kinetics, *Chemical Engineering Communications*, 203 (11), 1497-1506.
- Cheon Y.-H., Kim K.-J., Kim S.-H., 2005, A study on crystallization kinetics of pentaerythritol in a batch cooling crystallizer, *Chemical Engineering Science*, 60 (17), 4791-4802.
- De Haan A., Bosh H., 2013, *Industrial Separation Processes*, Walter de Gruyter GmbH, Berlin.
- Herndl G., 1982, *Stoffubergang in gerührten Suspensionen*, PhD Thesis, Technical University of Munich, Munich, Germany.
- Kaćunić A., Ćosić M., Rušić D., Kuzmanić N., 2017, Effect of impeller off-bottom clearance on crystal growth kinetics of borax in dual-impeller batch cooling crystallizer, *Chemical Engineering Transactions*, 57, 787-792.
- Kim K.-J., Mersmann A., 2001, Estimation of metastable zone width in different nucleation processes, *Chemical Engineering Science*, 56 (7), 2315-2324.
- Mersmann A., 1995, General prediction of statistically mean growth rates of a crystal collective, *Journal of Crystal Growth*, 147, 181-193.
- Mersmann A., 1994, *Crystallization Technology Handbook*, Marcel Dekker, New York.